# An Adaptive Fuzzy Logic Based Energy Management Strategy on Battery/Ultracapacitor Hybrid Electric Vehicles

He Yin, Wenhao Zhou, and Chen Zhao *Student Member, IEEE*, Mian Li* and Chengbin Ma *Member, IEEE*

***Abstract*—One of the key issues for the development of electric vehicles (EVs) is the requirement of a supervisory energy management strategy, especially for those with hybrid energy storage systems. An adaptive fuzzy logic based energy management strategy (AFEMS) is proposed in this paper to determine the power split between the battery pack and the ultracapacitor (UC) pack. A Fuzzy logic controller is used due to the complex real-time control issue. Furthermore, it does not need the knowledge of the driving cycle ahead of time. The underlying principles of this adaptive fuzzy logic controller are to maximize the system efficiency, to minimize the battery current variation, and to minimize UC state of charge (SOC) difference. NetLogo is used to assess the performance of the proposed method. Compared with other three energy management strategies, the simulation and experimental results show that the proposed AFEMS promises a better comprehensive control performance in terms of the system efficiency, the battery current variation, and differences in the UC SOC, for both congested city driving and high way driving situations.**

***Index Terms*—Batteries; ultracapacitors; fuzzy logic; adaptive; energy management strategy**

## NOMENCLATURE

| | |
|---|---|
| $\mu$ | Value of $i^{th}$ output level |
| $\mu_{crisp}$ | Crisp output value |
| $E_{DC}$ | Energy consumed by the driving cycle |
| $E_{Loss}$ | Total energy loss of the system |
| $E_{UC}$ | Energy storaged in the Ultracapacitor |
| $F_1$ | Criteria for system efficiency |
| $F_2$ | Criteria for battery current variation |
| $F_3$ | Criteria for UC SOC differences |
| $I\_BatP$ | Battery side DCDC output current |
| $I\_BatP$ | Current of the battery pack |
| $I\_UCP$ | Current of the UC pack |
| $I\_UCP$ | UC side DCDC output current |
| $I_{Bat}$ | Battery current in ALD method |
| $OCV$ | Open circuit voltage in battery |
| $r$ | Key adaptive parameter |
| $R_{l,UC}$ | Parallel resistor in battery |
| $R_{S,bat}$ | Series resistor in battery |
| $R_{S,UC}$ | Series resistor in battery |
| $SOC_{bat}$ | SOC of battery |
| $SOC_{bat}$ | SOC of battery |
| $SOC_{UC}$ | SOC of UC |
| $V\_BatP$ | Voltage of the battery pack |
| $V\_BatPDC$ | Battery side DCDC output voltage |
| $V\_UCP$ | Voltage of the UC pack |
| $V\_UCPDC$ | UC side DCDC output voltage |

Manuscript received December 11, 2015; revised February 5, 2016; accepted March 28, 2016.



This work is supported by the National Natural Science Foundation of China under Grant No. 51375302 (2014-2017).

H. Yin, C. Zhao, M. Li, and C. Ma are with University of Michigan-Shanghai Jiao Tong University Joint Institute, Shanghai Jiao Tong University, 800 Dongchuan Road, Minhang, Shanghai 200240, P. R. China (e-mail: yyy@sjtu.edu.cn; zc437041363@sjtu.edu.cn; mianli@sjtu.edu.cn; chbma@sjtu.edu.cn). M. Li and C. Ma are also with a joint faculty appointment in School of Mechanical Engineering, Shanghai Jiao Tong University. W. Zhou is with United Automotive Electronic Systems Co., Ltd., No. 555 Rongqiao Road, Shanghai, 201206, P. R. China (wenhao.zhou@uaes.com).

## I. INTRODUCTION

HYBRID electric vehicles (HEVs) using an internal combustion engine (ICE) and the motor(s) with a battery pack are the main portion of the renewable energy vehicles in the market at present (e.g., Toyota Prius, Honda Insight, Chevy Volt, etc.). All of them use a battery pack to supplement downsized conventional ICEs. However, HEVs still may not help people get rid of problems caused by burning of fossil fuel. It is believed that such HEVs are only the intermediate products between conventional ICE vehicles and battery electric vehicles (BEVs, which use batteries as the primary energy source without ICEs). With the rapid development of battery technologies, lithium-ion batteries today have reasonable energy density compared with other types of batteries but become much cheaper. It is possible to utilize them as the primary energy storage component for automotive applications. However, lithium-ion batteries still have disadvantages such as low power density, short cycle life, etc. On the other hand, a possible solution may be to select another energy storage component, ultracapacitor (UC), to assist batteries, forming a hybrid energy storage system (HESS) for EVs. UCs have high power density, long cycle life, quick dynamic response but low energy density, which are opposite towards batteries. So the combination of them is anticipated to complement one another [1], [2]. Currently HESSs are preferred because multiple design dimensions allow synergy among different energy sources and this kind of cooperation usually promises better vehicle system performance than those with a single-energy storage source. Since there are two dimensions for design in HESS, an energy management strategy (EMS) is required to optimize the performance of the HESS [3].

A literature survey shows that researchers in various areas have proposed different EMSs for different HESS structures.

Siang [4] classified the main proposed approaches of the energy management strategies into two categories: rule-based and optimization-based EMSs. Rule-based EMSs could be further classified as deterministic and fuzzy rule-based EMSs. They are favoured by automobile manufacturers because of their simplicity and effectiveness for real-time supervisory control. For example, energy control on Toyota Prius and Honda Insight are both based on a deterministic rule-based management strategy, called power follower control strategy [5]. In particular, a fuzzy rule-based EMS for battery/UC HESSs, which utilizes adaptive techniques, is proposed in this paper.

In research communities, some focus on using fuzzy logic based EMSs to control the power split between an ICE and a battery-supported electric motor [6]–[10]. The main goal of these EMSs is to level the operation points of the ICE onto its high efficiency curve with the complementary energy supplied by batteries in order to increase the ICE efficiency and decrease emission. Due to the complexity of HEVs, the fuzzy logic controller for an EV equipped with battery and UC packs should be more effect, accurate and easier to be implemented. For this reason, the control performance of a fuzzy logic controller for an EV should be better due to a much simpler power-train system. Some used fuzzy logic in a FC/battery dual energy source system [11]–[13]. They use batteries to capture the energy from regenerative braking and reduce transient response of fuel cells. The objective usually is to improve the system efficiency and maintain the battery state of charge (SOC) at a reasonable level. However, only few authors make use of fuzzy logic to develop EMSs for a battery/UC dual energy source system [14], [15], not mention an adaptive fuzzy logic based EMS. Besides, most of the mentioned approaches have their limitations: they use only one test driving cycle for simulations or experiments; the evaluation criteria are not standardized for EMS comparison; adaptiveness of the designed controllers are mostly not mentioned.

An adaptive fuzzy logic based energy management strategy (AFEMS) for a battery/UC hybrid energy storage system is proposed in this paper. The battery/UC HESS is a complicated multi-variable non-linear process and it is very hard, if not impossible, to define an exact mathematical model. It utilizes heuristic information for control and provides robust performance without the request of mathematical models [8], [16]. Also, the fuzzy logic controller does not have real-time calculation issues, which is critical for real-world vehicle applications. Therefore, the AFEMS is proposed as a convenient practical solution to such processes. Through the off-line optimization and on-line tuning of the membership functions, the AFEMS adaptively determines the optimal membership function according to the previous driving patterns. Multiple driving cycles with different driving patterns/characteristics are selected for the simulations and experiments to verify the effectiveness, efficiency and comprehensiveness of the proposed AFEMS. In addition to system efficiency, two more comparison criteria are defined for EMS evaluation, including battery current variation and the difference of UC SOC.

## II. System Configuration

### A. Vehicle Configurations

Parallel active topology is chosen for the vehicle system in this paper because it solves the DC link voltage matching problem among the battery pack, the UC pack and the load very well. Furthermore, the DC/DC converters are not supposed to be full rated in this topology, which makes it much easier to implement the experimental devices [17]. Fig. 1 shows the overview of the vehicle configuration. The battery pack and the UC pack together form a dual-energy storage system. The battery pack is connected with a unidirectional DC/DC converter while the UC pack is connected with a bidirectional DC/DC converter. The main reason of using this setup is because the entire regenerative energy should be absorbed by the UC pack while the battery pack are supposed to only supply energy but not absorb energy. The unidirectional DC/DC converter is used to implement the proposed EMS and the bidirectional DC/DC converter is used for DC link voltage stabilization. Solid lines in Fig. 1 represent the energy flow with arrows indicating the direction while the dashed lines represent the signal flow. During driving, the battery pack supplies the calculated current (power) according to the specified EMS implemented in the vehicle controller and the UC pack supplies the complementary current (power) to meet the demand of the driving cycle. The motor part is replaced by driving cycles in simulations and experiments which will be explained in this section later.

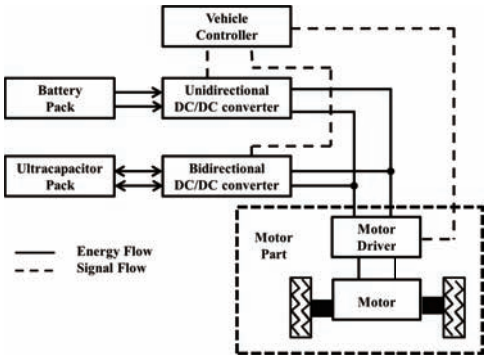


Fig. 1. Vehicle configurations.

### B. Battery and UC models

Lithium-ion battery is chosen for the HESS and the battery model used in this paper is shown in Fig. 2(a). It is composed of an ideal DC voltage source (OCV), a series resistor ($R_{S,bat}$), two additional resistor/capacitor pairs $R_1$/$C_1$ and $R_2$/$C_2$. The values of these elements are represented as sixth-order polynomial functions with respect to the SOC of the battery. For example:

$$R_{S,bat}(SOC) = 0.02 - 0.236SOC - 1.6899SOC^2 \\ -5.66SOC^3 + 9.67SOC^4 - 8.13SOC^5 + 2.67SOC^6, \quad (1)$$

$$OCV(SOC) = 2.3016 + 15.962SOC - 99.56SOC^2 + 295.2SOC^3 \\ -446.49SOC^4 - 331.41SOC^5 - 95.559SOC^6. \quad (2)$$

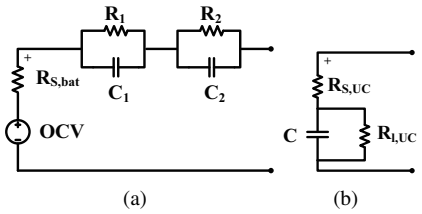


Fig. 2. (a) Battery model.(b) UC model.

Similarly, $R_1$, $R_2$, $C_1$ and $C_2$ are all represented by four sixth-order polynomial functions, whose coefficient values are summarized in Table I for simplicity, where $a_n$ is the coefficient of the nth-order term (n = 0,...,6). All coefficients are determined based on experimental data regression on a specific battery cell (Lishen Lithium-ion Power Cell of LP2770102AC-12.5Ah). The sixth-order polynomial function is used here because it can provide enough accuracy for real-time energy control according to the literature [18].

The UC model used in this paper is shown in Fig. 2(b), which consists of an ideal large-value capacitor ($C$), a parallel leakage resistor ($R_{l,UC}$), and an equivalent series resistor (ESR or $R_{S,UC}$). NIPPON CHEMI-CON N3ELD DLCAP Module is used in the simulations and experiments.

The detailed characteristics of the battery/UC cells and packs are summarized in Table VI according to the product manual.

TABLE I
COEFFICIENTS OF $R_1$, $R_2$, $C_1$ AND $C_2$.

| | $a_0$ | $a_1$ | $a_2$ | $a_3$ | $a_4$ | $a_5$ | $a_6$ |
|---|---|---|---|---|---|---|---|
| $R_1$ | 0.3469 | -3.555 | 13.81 | -25.05 | 21.49 | -7.028 | 0 |
| $C_1$ | -87.29 | 2052 | -9051 | 18400 | -17830 | 6635 | 0 |
| $R_2$ | 0.2484 | -3.991 | 27.3 | -89.26 | 149 | -122.3 | 39.08 |
| $C_2$ | -523.6 | 17740 | 52440 | -561400 | 1475000 | -1618000 | 641600 |

Another point that needs to be mentioned is the definition of State of Charge (SOC). The general definition of SOC is defined by (3) and the SOC of batteries is usually calculated by Ampere-hour integration as shown in (4) [19], where $Q_{nominal}$ is the battery rated capacity, and $t_0$ represents the initial time.

$$SOC(t) = \frac{Q(t)}{Q_{nominal}}, \tag{3}$$

$$SOC_{bat}(t) = SOC_{bat}(t_0) + \frac{1}{Q_{nominal}} \int_{t_0}^{t} i_{bat}(\tau) d\tau. \tag{4}$$

For capacitors, we have:

$$Q = V \cdot C. \tag{5}$$

Therefore the SOC of capacitors can be defined as (6), where $V_{nominal}$ is the UC rated voltage.

$$SOC_{UC}(t) = \frac{V(t) \cdot C}{V_{nominal} \cdot C} = \frac{V(t)}{V_{nominal}}. \tag{6}$$

$$E_{UC} = 0.5 \cdot C \cdot V^2. \tag{7}$$

Furthermore, energy stored in an UC is proportional to the square of its voltage as shown in (7). If $SOC_{UC}$ of a capacitor reaches 0.5 from 1, 75% of the stored energy is dissipated. As a result, a capacitor is considered to be fully discharged when $SOC_{UC}$ decrease to 0.5 from 1 and the half nominal voltage is defined as the cut-off voltage of an UC.

### C. DC/DC converter models

In order to solve the problem associated with DC link voltage matching and to implement the proposed EMS, DC/DC converters are used [20].

A boost DC/DC converter is utilized as the unidirectional converter because of the low voltage of the battery pack. Fig. 3 shows its steady-state equivalent circuit, which mainly consists of a smoothing inductor (L), a diode (D), a capacitor (C) and a switch (S).

On the other hand, a buck-boost DC/DC converter is utilized as the bidirectional DC/DC converter. Fig. 4 shows its steady-state equivalent circuit, mainly including a smoothing inductor (L), a capacitor (C) and two switches (S). Detailed parameter values are shown in Table II, where L is the inductance of the inductor, $R_L$ is the resistance of the inductors, $R_S$ is the resistance of switches, $V_D$ is the threshold voltage of diodes and $R_D$ is the equivalent resistance of diodes. The operation frequency of switches is 20 $kHz$.

Moreover, the efficiency of both converters can be represented as (8) and (9), respectively. Meanwhile, efficiency maps of both converters are shown in Fig. 5. It could be noticed that even from the energy conversion efficiency perspective, it is recommended to have a smaller current which means the higher DC/DC converter efficiency.

$$\eta_{uni} = 1 - \frac{I^2\_BatP \cdot R_L + D(I^2\_BatP \cdot R_S)}{V\_BatP \cdot I\_BatP}, - \frac{(1-D)(I^2\_BatP \cdot R_D + V_D \cdot I\_BatP)}{V\_BatP \cdot I\_BatP}, \tag{8}$$

$$\eta_{bi} = 1 - \frac{I^2\_UCP \cdot R_L + I^2\_UCP \cdot R_S}{V\_UCP \cdot I\_UCP}. \tag{9}$$

TABLE II
SPECIFICATIONS OF DC/DC CONVERTERS

| Parameter | Value | Unit |
|---|---|---|
| $L$ | 200 | $\mu H$ |
| $R_L$ | 0.1 | $\Omega$ |
| $R_S$ | 0.005 | $\Omega$ |
| $V_D$ | 0.26 | $V$ |
| $R_D$ | 0.012 | $\Omega$ |
| $f_S$ | 20 | $kHz$ |

### D. Vehicle dynamics and driving cycles

Driving cycles which represents driving patterns in a region or city are used to replace the load in both simulations and experiments [21]. They are usually speed-time profiles, which need to be converted to corresponding power-time profiles. In this paper, the vehicle parameters of i-MiEV listed in

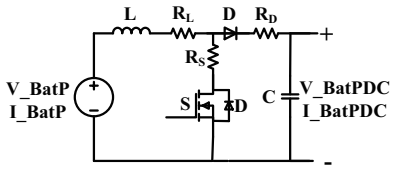


Fig. 3. Unidirectional DC/DC converter model.

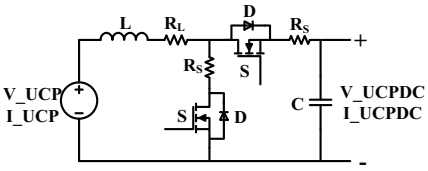


Fig. 4. Bidirectional DC/DC converter model.

Table III is used for this transformation. By applying simplified longitudinal vehicle dynamics, driving cycles in velocity could be converted into driving cycles in power demands [1], [22]. Driving cycle profiles are scaled down by 200 since i-MiEV is equipped with a 16 $kWh$ battery pack while an 80$Wh$ battery pack is used in the experiment.

TABLE III
CHARACTERISTICS OF THE VEHICLE

| Parameter | Value | Unit |
|---|---|---|
| Empty vehicle weight | 1100 | $kg$ |
| Rolling Coefficient $\mu$ | 0.01 | |
| Battery capacity | 16 | $kWh$ |
| Maximum speed | 130 | $km/h$ |
| Air density $\rho$ | 1.2 | $kg/m^3$ |
| Drag Coefficient $C_d$ | 0.24 | |
| Front Area $A$ | 2.17 | $m^2$ |

Ten commonly used driving cycles are utilized in the development of the AFEMS, including JC08, NEDC, NYCC, UDDS, US06, HWFET, IM240, FTP, La92, and SC03 [23]. The selected driving cycles have different driving patterns. For example, JC08 Driving Cycle typically represents driving in congested city traffic while HWFET represents a highway traffic situation. The opposite driving patterns are confirmed by speed-time profiles shown in Fig. 6(a) and (b). Both of them are used as test driving cycles in the evaluation to verify the adaptiveness and performance of the proposed EMS.

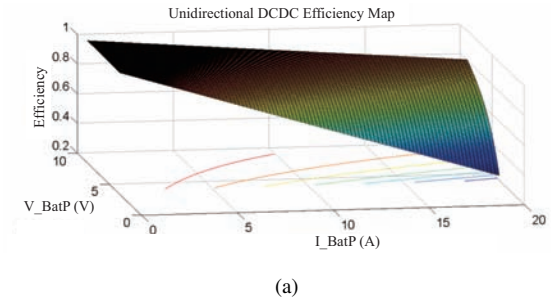


Fig. 5. DC/DC converter efficiency maps (a) Unidirectional DC/DC converter. (b) Bidirectional DC/DC converter.

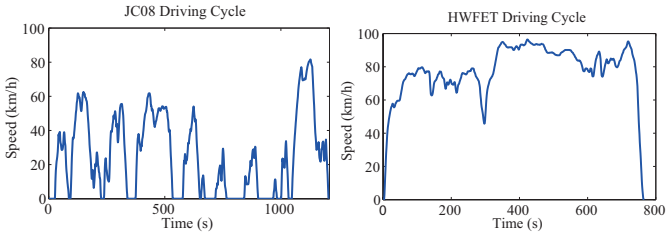


Fig. 6. Example speed-time profiles (a) JC08 driving cycle.(b) HWFET driving cycle.

### *E. Sizing of the UC pack*

Since the size of the battery pack has been determined in the previous section (80$Wh$), the size of the UC pack still needs to be determined to match the system. According to the principle No.3 discussed in the next section, the UC pack is actually working as an energy buffer. In order to deal with the possible unexpected future load, it is recommended to maintain the energy level of the UC to be 50% [18]. Thus 50% energy of the UC pack should be able to cover the largest peak power for all possible driving cycles [15]. According to the driving cycle classification discussed in Section III.C, the largest peak power, existing in NEDC, determines the required UC pack energy level, 16$Wh$. Note that the volume of the UC pack may be relatively large for i-MiEV. This is because that this paper focuses on the adaptive FLC strategy. It requires analyzing a large amount of different kinds of driving cycles which includes high-way driving cycles. Small size electric vehicles, such as i-MiEV, are not suitable for such kinds of driving cycles. While, the UC pack here should supply these peak powers and therefore the size of the UC pack is relatively large in this work.

## III. AN ADAPTIVE FUZZY LOGIC BASED ENERGY MANAGEMENT STRATEGY

In this section, the underlying principles of the proposed AFEMS are presented first, followed by the comparison criteria used for the evaluation of different EMSs. Finally, the AFEMS is developed and its details are discussed.

### *A. Underlying principles*

In the design process of an EMS, no matter what discipline or theorem it is developed from, foundational principles (constraints) should always be kept in mind. There are three basic

principles under consideration during the development of the proposed EMS.

**Principle No. 1**

The power demand of the driving cycle should be satisfied consistently. Even though the propulsion system and usage scenario might be different, EVs should be able to 'run' like conventional vehicles, i.e., driving an EV should at least not 'feel' different from driving a conventional vehicle. So, the required driving pattern (driving cycles in simulations and experiments) should always be achieved.

**Principle No. 2**

Battery lifetime, efficiency and state of health (SOH) are largely dependent on working conditions, including the absolute value of the battery current and current dynamics of batteries. It has been well-known that large discharging current would significantly increase energy loss on the battery internal resistor, which leads to high working temperature, low battery efficiency and short cycle life. Also, large variation in the discharging current would lead to damage to batteries, which also means short battery lifetime and poor SOH. In [17], the author shows that pulse load leads to higher temperature increasing compared to a constant average load. Therefore, the battery current should be kept in a low absolute level and stable as much as possible. A battery-alone energy storage system is unable to relieve the stress on batteries no matter which kind of EMSs is applied; which is also the reason why UC cells should be taken into consideration.

**Principle No. 3**

It is also important to notice that batteries should be the only real 'energy' sources on the vehicle. Given properties of batteries and UCs, the energy demanded by the driving cycle should be supplied by the energy from batteries only, and UCs should be used as energy buffers. That is, UCs are 'power' sources. The purpose of using UCs is to reduce and guarantee a much smoother load profile of the battery pack and they are never expected to provide net energy just like what the batteries function. Ideally, the SOC of a UC cell at the end of a trip is expected to be the same as that at the beginning of the trip, which means energy stored in the UC cell is not consumed.

### *B. Comparison criteria*

In order to evaluate the performance of an EMS, comparison criteria should be determined. The most important aspect that should always be considered is the system efficiency. Many researchers have taken the system efficiency as the criterion in their evaluations [24]–[26]. In terms of the HESS discussed in this paper, (10) holds true based on system energy conservation, where $E_{DC}$ is the energy consumed by the driving cycle, $E_{BatteryPack}$ is the net energy supplied by the battery pack, $E_{UCPack}$ is the net energy supplied by the UC pack, and $E_{Loss}$ is the total energy loss of the system. In this formulation, $E_{Loss}$ contains four parts, as shown in (11): $E_{BatteryPackLoss}$ is the energy loss caused by the battery internal resistors; $E_{UCPackLoss}$ is the energy loss caused by UC internal resistors; $E_{UniDCDC}$ is the energy loss caused by the unidirectional DC/DC converter, and $E_{BiDCDC}$ is the energy loss caused by the bidirectional DC/DC converter. Therefore, the first criterion $F_1$ on the system efficiency is defined as in (12), which is expected to be as high as possible.

$$E_{DC} = E_{BatteryPack} + E_{UCPack} + E_{Loss}, \quad (10)$$

$$E_{Loss} = E_{BatteryPackLoss} + E_{UCPackLoss} + E_{UniDCDC} + E_{BiDCDC}, \quad (11)$$

$$F_1 = \frac{E_{DC}}{E_{BatteryPack} + E_{UCPack} + E_{Loss}}. \quad (12)$$

However, using the system efficiency only is not enough. It has been shown that the frequent current variation would dramatically reduce the lifetime of a lithium-ion battery [18]. Given this observation, the amount of battery current variation should also be considered in the evaluation. For simplicity, only the current from the battery pack ($I\_BatP$) is considered instead of a single battery cell. At each time step, the current difference between adjacent time steps is recorded as an array. At the end of a driving cycle, the L-2 norm of this n-dimensional array is defined as the second criterion $F_2$ as shown in (13). A large $F_2$ value implies that the battery pack may cover too much dynamic current.

$$F_2 = \sqrt{\sum_{i=1}^{n} (I\_BatP_i - I\_BatP_{i-1})^2}. \quad (13)$$

How much energy is consumed from or transposed into the UC pack is considered in $F_3$ as shown in (14) given the fact that the UC pack is supposed to be the power source instead of energy source. This criterion is achieved by monitoring the SOC difference of the UC cell between the initial state $SOC_{UC}(t_0)$ and final state $SOC_{UC}(t_f)$. If the UC SOC is unchanged, it perfectly serves as an energy buffer. However, it is really hard to realize the perfect situation. Thus $F_3$ should be as small as possible.

$$F_3 = |SOC_{UC}(t_0) - SOC_{UC}(t_f)|. \quad (14)$$

### *C. Adaptive fuzzy logic based energy management strategy*

The block diagram of the proposed battery/UC HESS energy flow controller is shown in Fig. 7. 'Driver Command Interpreter' is to convert driver commands and vehicle speeds into power demands. 'Driving Mode Detector' is used to decide driving modes as specified in Fig. 11, which will be explained later. 'AFEMS Controller' has three inputs: power demands from the Driver Command Interpreter; vehicle driving modes from the Driving Mode Detector; and UC SOC which reflects the states of the HESS. Note that the battery is considered as a long-term energy supplier in this paper and thus its SOC only affects the system efficiency slightly. Therefore, only the UC SOC is used to indicate the states of the HESS. The output of the AFEMS Controller is the battery pack output current which is used as a reference signal for the control of the HESS. This reference signal, together with the

power demand, decides how the energy storage components in the HESS act and how their SOC changes respectively.

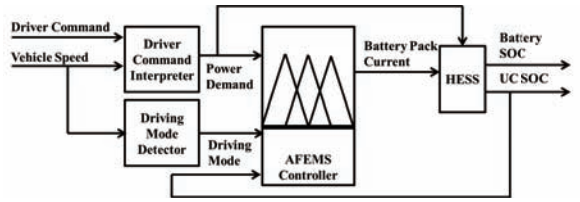


Fig. 7. Block diagram of the proposed AFEMS controller.

Generally, the AFEMS Controller works with three procedures: fuzzification of inputs, inference mechanism, and defuzzification of outputs, as shown in Fig. 8 [16].

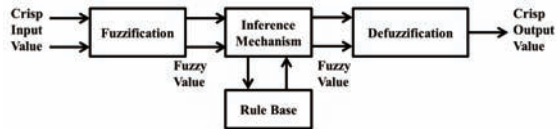


Fig. 8. AFEMS controller.

**Procedure 1: Fuzzification**

In fuzzy logic, the membership function is used to convert the crisp inputs into fuzzified inputs. The crisp input in the proposed AFEMS is the power demand from the vehicle and the UC SOC. Fig. 9 shows the membership function of the power demand. It converts the crisp power into fuzzy levels.

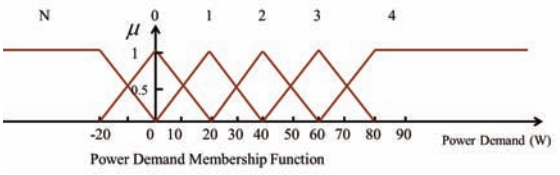


Fig. 9. Membership function of power demand.

In this paper, the power demands are divided into five categories: 'N', '0', '1', '2', '3', '4', and each of them has its own $\mu$ value. For example, when the power demand is $30W$, the $\mu$ values of 'N', '0', '3' and '4' are all 0, and the $\mu$ values of '1' and '2' are both 0.5. Similarly, the membership function of another crisp input UC SOC, is shown in Fig. 10. It converts the crisp UC SOC into fuzzy levels too.

The UC SOC is divided into three categories: 'Low', 'Medium' and 'High', and each of them has its own $\mu$ value as well. For example, in this paper when the UC SOC is 0.65, the corresponding $\mu$ value of 'Low' is 0.5, $\mu$ value of 'Medium' is 0.5 and $\mu$ value of 'High' is 0.

**Procedure 2: Inference Mechanism**

After the fuzzified inputs are obtained, in inference mechanism, rule base is used to obtain fuzzy conclusions. This part is more like an expert system because experience and heuristic information are used for control decision making. Before the rule base is set up, in the proposed AFEMS, vehicle speeds are divided into four categories in order to divide a single large rule base into four parallel sub-rule-bases.

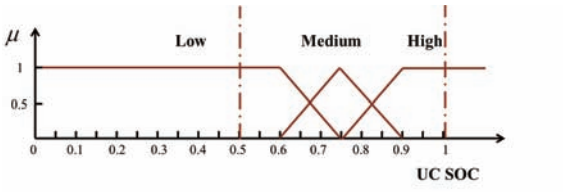


Fig. 10. Membership function of UC SOC.

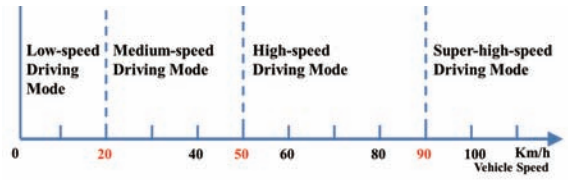


Fig. 11. Driving mode classification.

As shown in Fig. 11, we define four driving modes: Low-Speed (LS) Mode, Medium-Speed (MS) Mode, High-Speed (HS) Mode and Super-High-Speed (SHS) Mode according to different vehicle speeds. Then four sub-rule-bases are defined for those four driving modes, respectively, as shown in Table IV. Note that in order to avoid tedious rule tables, the sub-rule-bases tables only contain two degrees of freedom, i.e., the vehicle speed and UC SOC.

TABLE IV
FOUR SUB-RULE-BASES

(a) Low-speed Mode Rule Base

| $I\_BatP$ Level | | Power Demand Level | | | | | |
|---|---|---|---|---|---|---|---|
| | | N | 0 | 1 | 2 | 3 | 4 |
| UC SOC | L | 1 | 1 | 2 | 2 | 3 | 3 |
| | M | 0 | 1 | 1 | 2 | 2 | 3 |
| | H | 0 | 0 | 1 | 1 | 2 | 2 |

(b) Medium-speed Mode Rule Base

| $I\_BatP$ Level | | Power Demand Level | | | | | |
|---|---|---|---|---|---|---|---|
| | | N | 0 | 1 | 2 | 3 | 4 |
| UC SOC | L | 1 | 2 | 2 | 3 | 3 | 4 |
| | M | 1 | 1 | 2 | 2 | 3 | 3 |
| | H | 0 | 1 | 1 | 2 | 2 | 3 |

(c) High-speed Mode Rule Base

| $I\_BatP$ Level | | Power Demand Level | | | | | |
|---|---|---|---|---|---|---|---|
| | | N | 0 | 1 | 2 | 3 | 4 |
| UC SOC | L | 2 | 2 | 3 | 3 | 4 | 4 |
| | M | 1 | 2 | 2 | 3 | 3 | 4 |
| | H | 1 | 1 | 2 | 2 | 3 | 3 |

(d) Super-High-speed Mode Rule Base

| $I\_BatP$ Level | | Power Demand Level | | | | | |
|---|---|---|---|---|---|---|---|
| | | N | 0 | 1 | 2 | 3 | 4 |
| UC SOC | L | 2 | 3 | 3 | 4 | 4 | 5 |
| | M | 2 | 2 | 3 | 3 | 4 | 4 |
| | H | 1 | 2 | 2 | 3 | 3 | 4 |

The conclusions drawn from these rule bases are the fuzzified battery pack current levels, which are represented by six levels '0','1','2','3','4','5'. For example, when the vehicle speed is 40 $km/h$, i.e., it is in MS Mode, the second table is picked up as the rule base. Meanwhile, if the $\mu$ values of 'Low', 'Medium' and 'High' are 0.5, 0.5 and 0 in terms of UC SOC levels and the $\mu$ values of 'N','0','1','2','3','4' are 0, 0.5, 0.5, 0, 0, and 0 in terms of power demand levels, the $\mu$ values of '0','1','2','3','4','5' in terms of fuzzified battery

pack current levels are 0, 0 , 0, 0.5, 0.5 and 0 respectively. Obviously, it could be noticed that basically a larger power demand or lower UC SOC state leads to a larger battery pack current level.

**Procedure 3: Defuzzification**

The output membership function is defined for converting the fuzzified outputs to crisp outputs as shown in Fig. 12(a). Many methods could be utilized for defuzzification. The center of gravity (COG) method is the most common one in practice and is used in this paper as shown in (15) [19].

$$\mu^{crisp} = \frac{\sum_i b_i \int \mu_i}{\sum_i \int \mu_i}, \tag{15}$$

where $b_i$ denotes the center of the membership function for the consequent of rules, $\mu$ is the value of $i^{th}$ output level and $\mu_{crisp}$ is the crisp output value.

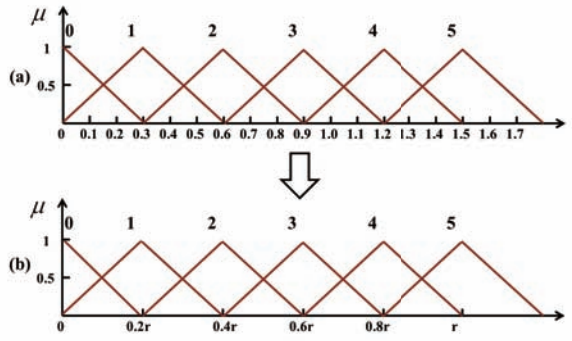


Fig. 12. (a) Membership function of battery pack current. (b) Adaptive output membership function.

In order to achieve better control performance, the output membership function is made periodically refreshed in this paper based on historical driving cycle information. In other words, the controller should be adaptive to varying driving patterns. This is achieved by converting the output membership function shown in Fig. 12(a) into the one shown in Fig. 12(b). Therefore, the past driving cycle information is considered in the defuzzification membership function. Here, the parameter $r$ shown on the membership function is no longer a constant as shown on Fig. 12(a); its value changes according to the information of the past driving cycle. Here the $r$ value is a key parameter that needs to be determined adaptively using the off-line optimization and on-line update technology. The decision making procedure of the $r$ value consists of two off-line steps and two on-line steps. The basic idea is to analyze pieces of short driving cycles (called 'sub-driving-cycles' in this paper) derived from the commonly used driving cycles, and to find the optimal parameter values for each of them given different driving conditions (different UC SOCs and driving modes). Then the optimal parameter values as well as the corresponding driving conditions are stored in the form of rule tables. Once the vehicle is on the road, the controller assigns the parameter value by referring to the chosen rule tables. The details of the procedure are given as follows.

**Step1: Off-Line Driving Pattern Recognition**

Ten common test driving cycles are gathered as mentioned in the previous section, which can cover diverse driving patterns. For example, JC08 features congested city driving conditions and HWFET represents highway driving conditions. Eight of ten, NEDC, NYCC, UDDS, US06, IM240, FTP, La92, and SC03, are used in this step and each of these eight driving cycles is split into 100s-long equal length sub-driving-cycles (SDCs). Thus 154 SDCs are obtained. Note that these 154 SDCs should be able to cover most of the possible patterns. If there exists a special driving profile whose patterns are not similar to anyone of SDCs, this fuzzy logic controller will still work but possibly with a relative lower efficiency. In this regard, this special driving profile should be added into this pattern recognition procedure. Three of them are shown in Fig. 13 including No.49 SDC, No.92 and No.143 SDC, and they apparently show different driving patterns. After that, every SDC is quantitatively analyzed with forty-four driving pattern parameters [23]. These driving pattern parameters can well characterize the driving cycles.

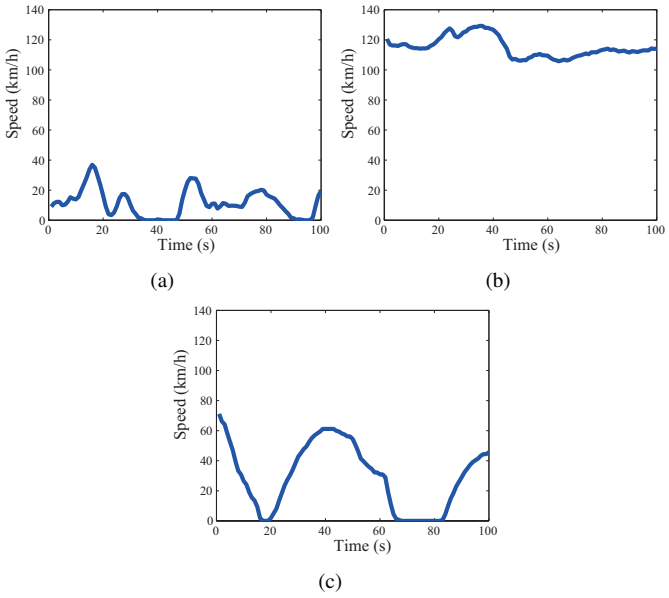


Fig. 13. (a) No.49SDC.(b) No.92 SDC. (c) No.143 SDC.

**Step2: Off-Line Optimal Parameter Tuning**

The second step is to determine an optimal $r$ value which gives the highest system efficiency for each SDC under different driving situations (i.e., different driving modes and different initial UC SOCs). An iterative seeking procedure using the computer simulation must be implemented in order to properly decide the optimal $r$ value and Fig. 14 shows the flow chart of this iterative procedure.

Principle No.3 in the previous section emphasizes that UCs are supposed to provide no net energy, or as little as possible. Therefore, one constraint during the optimal parameter tuning procedure is that: the UC SOC difference between the beginning of a driving cycle and the end of the same driving cycle should be as small as possible and here the upper bound of this difference is set to be 0.1. Table V shows the optimal parameter tuning results of No.71 SDC. The value 2.1 on the northwest corner means that if the vehicle is in Low-Speed

Mode and the UC SOC is 0.55 at present, the optimal value of $r$ for the output membership function is 2.1. Note that the first two steps are conducted off-line, thus their computational efforts will not affect the efficiency of the proposed AFEMS.

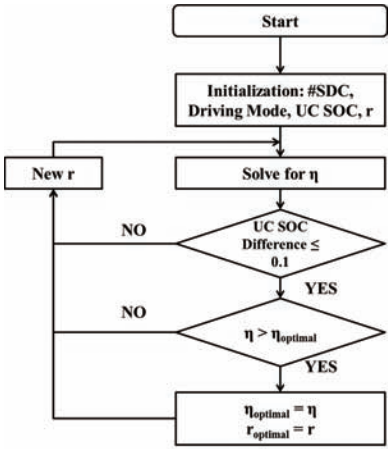


Fig. 14. Flow chart of the optimal parameter finding procedure.

TABLE V
OPTIMAL PARAMETER TUNING RESULTS OF NO. 71 SDC

| | LS Mode | MS Mode | HS Mode | SHS Mode |
|---|---|---|---|---|
| 0.55 | 2.1 | 1 | 1 | 0.7 |
| 0.6 | 1.5 | 0.8 | 0.8 | 0.5 |
| 0.65 | 1.2 | 0.7 | 0.6 | 0.4 |
| 0.7 | 0.9 | 0.6 | 0.4 | 0.4 |
| 0.75 | 0.7 | 0.7 | 0.3 | 0.3 |
| 0.8 | 0.7 | 0.5 | 0.3 | 0.3 |
| 0.85 | 0.8 | 0.4 | 0.3 | 0.2 |
| 0.9 | 0 | 0.3 | 0.3 | 0.2 |
| 0.95 | 0 | 0.3 | 0.3 | 0.1 |

**Step3: On-line Driving Feature Learning**

Through Off-Line Driving Pattern Recognition and Off-Line Optimal Parameter Tuning, there generates 154 44-dimension vectors representing the driving patterns of each SDC and 154 $9 \times 4$ matrix tables representing optimal parameters for each SDC under different driving situations. When it is during on-line driving, the last recorded 100s-long driving cycle is analyzed by checking the 44 pattern parameters. The AFEMS controller aims to find out the most similar one among those 154 SDCs and the optimal parameter tuning result of that SDC is going to be applied considering the instant driving mode and UC SOC level.

**Step4: On-line Driving Parameter Adjusting**

Although optimal parameters are found in previous steps, there still exist two issues which may make them sub-optimal. First, only a similar SDC could be found, not the identical SDC in most cases. Secondly, even an identical SDC is found, the optimal parameter value is chosen according to the previous 100s long driving cycle. It may not be true that the future driving cycle will still behave the same as the previous 100s-long part. Therefore the variation in the UC SOC would probably be bigger or smaller than what is expected, which validates the underlying Principle No.3. To solve this problem, the $r$ value needs to be adjusted by monitoring the control performance. If the UC SOC increases, $r$ needs to become smaller; otherwise $r$ needs to become larger. The redefined formula for $r$ is shown as follows,

$$r(t_k) = r_{optimal}(t_k) \cdot (1 + PN \cdot \frac{|SOC_{UC}(t_k) - SOC_{UC}(t_{k-1})|}{t_k - t_{k-1}} \cdot (SOC_{UC}(t_0) - SOC_{UC}(t_k)). \quad (16)$$

where $r(t_k)$ is the parameter value at the time step $k$; $r_{optimal}(t_k)$ is the off-line optimal parameter value; $PN$ is the penalty term; $SOC_{UC}(t_{k-1})$ is the UC SOC at the time step $k$; $SOC_{UC}(t_{k-1})$ is the UC SOC at time step $k-1$; $SOC_{UC}(t_0)$ is the initial UC SOC.

Finally, the control frequency of the controller should be determined carefully because it is related to battery current dynamics. High control frequency would lead to frequent battery current variation, which is negative for battery health. On the contrary, low control frequency makes it hard for the HESS to satisfy the driving cycle consistently (e.g., the UC SOC would possibly become too high or too low between two control steps). Therefore, how to choose an appropriate control frequency is a vital issue. Again, one of the underlying principles is that UCs are only regarded as the energy buffers and the UC SOC should be as stable as possible. So the control frequency is determined in the following way: a control instant will be effective if and only if the change of the UC SOC exceeds a threshold and this makes the control frequency adaptive to the UC SOC variation.

## IV. RESULTS AND ANALYSIS

The simulation platform is briefly introduced first in this section, followed by simulation results from AFEMS and other benchmark rule-based EMSs. Then experimental results are used to validate the simulation model and the effectiveness of the proposed AFEMS.

### A. Simulation environment

Although each battery cell and UC cell share certain similarities as energy storage units, they are very different in their dynamic behaviors. Also, their parameters are always slightly different from the nominal value. To better model those different behaviors and interactions among those different components, a multi-agent based simulation tool, Netlogo [27], is used in this paper.

### B. Simulation result and analysis

In order to verify the proposed AFEMS, several EMSs proposed in the literature are implemented as benchmarks. The limited tolerance method (LTM) is an EMS for battery/UC HESSs [28], whose main idea is to use UCs with batteries to achieve battery stress reduction as well as EV range extension. The thermostat method (TM) [29] is a conventional control method originally applied for HEVs, but the idea also works for BEVs. The average load demand (ALD) method [26] is a control method which sets the battery current to be constant for the entire driving process and ensures the initial and the terminal voltages of the UC pack to be the same. This method is considered to be the best EMS so far for battery/UC HESSs, as long as the driving cycle is known or given in advance.

The battery current in ALD could be calculated as shown as follows,

$$I_{Bat} = \frac{\int P_{dc}(t)dt}{T \cdot V_{BUS}}. \quad (17)$$

where $P_{dc}(t)$ is the power demand at time $t$, $T$ is the total trip length, and $V_{BUS}$ is the DC link voltage.

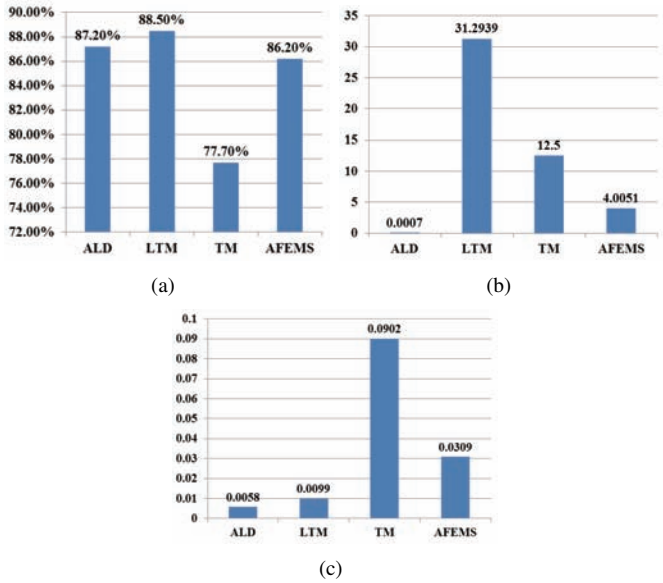


Fig. 15. Simulation results comparison of four EMSs (JC08) (a) System efficiency.(b)Battery current variation. (c) UC SOC difference.

The first testing driving cycle is JC08 which represents a congested city driving condition. It has been repeated four times to make the test long enough. Fig. 15 shows the simulation results of ALD, LTM, TM, and the proposed AFEMS. It can be seen obviously in Fig. 15(b) that LTM gives too large $C_2$ value. (i.e., the battery current variation is rather huge, which can be confirmed by the LTM current plot shown in Fig. 16). The system efficiency of TM is the lowest among the four EMSs as shown in Fig. 15(a). Furthermore, it is clear that the difference of UC SOC in TM is the highest as shown in Fig. 15(c). ALD is supposed to be the best EMS for a battery/UC HESS based BEV, which is also confirmed by the simulation results (i.e., the second best system efficiency and best for all other criteria). However, it should be noticed that the implementation of ALD is based upon the fact that the driving cycle is exactly known or given in advance, which is impossible for real-world applications. The proposed AFEMS shows good comprehensive performance under this congested city driving situation: it gets the third place in the system efficiency (only a little bit worse than the best one). The battery current variation is much better than the benchmarks expect ALD. The difference of UC SOC is also within the limitation. In general, its performances in all criteria are very close to those of ALD and most importantly it needs no driving cycle information in advance.

Fig. 16 shows the battery/UC pack current plots and UC pack voltage plots with different EMSs. Fig. 16(a) shows the battery/UC pack current plots using different EMSs and the red curve is the UC pack current curve while the blue one is the battery pack current curve. Fig. 16(b) shows the UC pack voltage plots. As shown in Fig. 16(a), the battery current of the LTM covers too many dynamic parts which leads to a larger battery current variation. Meanwhile, the battery current of TM is insensitive to the UC SOC which leads to a large variation of the UC SOC (referring to Fig. 16(b)). The ALD is supposed to be the best EMS because the entire driving cycle is given in advance. It is clear that when AFEMS is applied, the battery pack current is kept as low as possible with limited current variations, just like what can be seen in ALD; and the dynamic components are all most covered by the UC pack. In addition, the UC SOC is kept relatively stable.

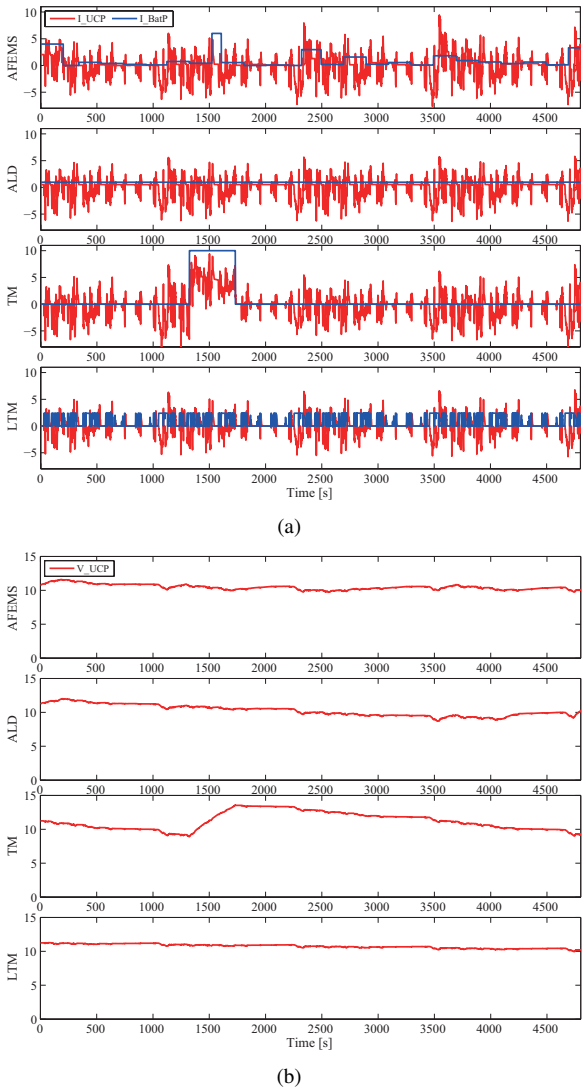


Fig. 16. Current and Voltage Plot of four EMSs (JC08) (a) Current plots.(b)Voltage plots.

The second test driving cycle is HWFET which represents highway driving conditions. It is also repeated four times to make the test enough long. Fig. 17 shows the simulation results of the ALD, LTM, TM, and the proposed AFEMS. In the simulation, LTM fails to work for this highway driving cycle because the battery pack is exhausted before the driving cycle

is over. Therefore, all the criteria for LTM are left empty here. TM shows the lowest system efficiency, highest battery current variation, and biggest UC SOC difference. So it is clear that TM gives the worst performance. Again, apart from battery current variation, AFEMS shows very close performances in all other three criteria compared with those of ALD. So the comprehensive control performance of AFEMS is also satisfying in terms of the highway driving situation.

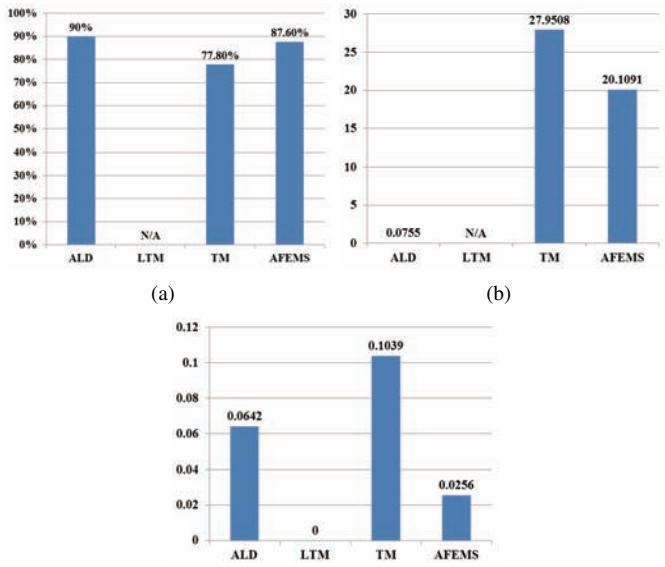


Fig. 17. Simulation results comparison of four EMSs (HWFET) (a) System efficiency.(b)Battery current variation. (c) UC SOC difference.

Fig. 18 shows the battery/UC pack current plots and UC pack voltage plots for different EMSs (expect LTM). These plots also confirm the conclusion that AFEMS provides reasonable battery current variation. Furthermore, the UC SOC is kept more stable than that in TM.

### C. Experimental result and analysis

An hardware-in-loop (HIL) experiment is used to validate the simulation model and proposed AFEMS. The test bench is shown in Fig. 19, including battery cells, UC cells, power supply, electronic load, DC/DC converters and a host computer. The EMSs are implemented on the host computer using LabVIEW; NI CompactRIO module is used to control the DC/DC converters; the power supply and the electronic load is used to emulate the test driving cycle. The detail specifications for the test bench are given in Table VI.

Fig. 20 shows the battery current plot and UC pack voltage plot for JC08 and Fig. 21 shows those for HWFET. Blue curve represents the simulation results and the red curve represents experimental results.

The error between simulation and experimental results when using ALD is summarized in Table VII. All of the four errors are all less than 5%, which means the simulation model is well developed.

However, simulation and experimental results show different battery current plot when AFEMS is applied, as shown in

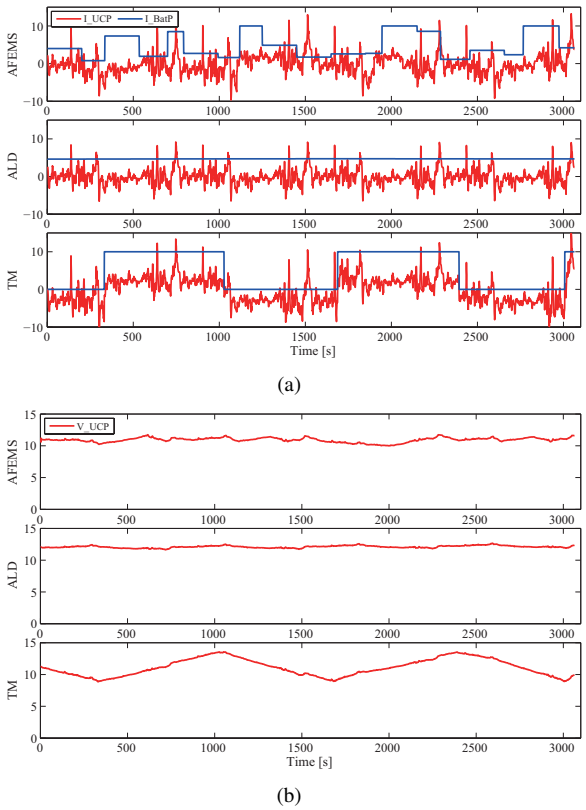


Fig. 18. Current and voltage plot of four EMSs (HWFET) (a) Current plots.(b)Voltage plots.

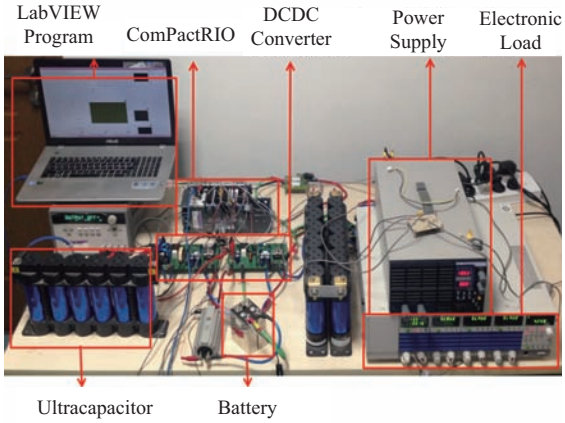


Fig. 19. Test bench.

Fig. 20(a) and Fig. 21(a). This is because the fuzzy rule-based control method is sensitive to the system conditions. Tiny deviation between simulation model and real device would lead to different control output. As the time goes on, the simulation model shows greater deviation from the real system, which leads to different AFEMS control results. And this difference further contributes to the next difference. However, the idea is that even this kind of difference happens, the trend of the control strategy decided by AFEMS shares similarity and the control performance is not influenced. As show in Table VIII, in both congested city and highway driving

TABLE VI
SPECIFICATIONS FOR THE TEST BENCH

| | |
|---|---|
| Battery Pack<br>(Lishen LP2770102AC)<br>Cut-off Voltage: 2.0V/cell | Two cells (series), 40Wh/cell<br>Nominal Voltage: 3.2V/cell<br>Mass : 370g/cell |
| UC Pack<br>(Nippon Chim-con DLE series)<br>Mass : 590g/cell<br>$R_l$ : $2M\Omega$/cell | Eight cells (8 Series) 2Wh/cell<br>Rated Voltage : 2.5 V/cell<br>Capacitance : 2300F/cell<br>ESR/$R_S$ : $1.2m\Omega$/cell |
| Electronic Load<br>(Kikusui PLZ-50F/150U) | Max Power:600W(1 PLZ-50F, 4 PLZ<br>150Us with 1.5-150V 0-30A each) |
| Power Supply<br>(TaKasago ZX-800L) | Max Power:800W<br>(0-80V,0-80A) |
| Controller<br>(NI- CompactRIO) | Onboard Clock: 40MHz<br>Cards: NI 9219, NI 9401 |

TABLE VII
ERROR SUMMARY (ALD)

| | JC08 | HWFET |
|---|---|---|
| I_BatP | 2.31 % | 0.58 % |
| V_UCP | 1.47 % | 3.43 % |

situation, the simulation and experiment results generally agree to each other.

## V. Conclusion

This paper presents an energy management strategy for a battery/UC hybrid energy storage system. Battery and UC are combined together in a parallel active topology because they have complementary characteristics. An adaptive fuzzy logic based EMS is developed to split the power requirement between batteries and UCs. Three underlying principles are followed during the development of the proposed AFEMS. Multi-agent simulation and hardware-in-loop experiment are involved in the design and verification. System efficiency, battery current variation, and UC SOC difference are taken as the criteria for EMS evaluation. Simulation results show that the proposed AFEMS leads to better comprehensive control performances than other benchmark EMSs while it does not need the driving cycle information in advance. Experimental results confirm the simulation model and show that the AFEMS is sensitive to system states so simulation and experiment provide different but similar control outputs. Even with the slight difference, it still presents good control performance in all three comparison criteria.

## References


[1] R. Sadoun, N. Rizoug, P. Bartholomeus, B. Barbedette, and P. Le Moigne, "Optimal sizing of hybrid supply for electric vehicle using li-ion battery and supercapacitor," in *Vehicle Power and Propulsion Conference (VPPC), 2011 IEEE*, Sept 2011, pp. 1–8.

[2] Amin, R. Bambang, A. Rohman, C. Dronkers, R. Ortega, and A. Sasongko, "Energy management of fuel cell/battery/supercapacitor hybrid power sources using model predictive control," *IEEE Trans. Ind. Informat.*, vol. 10, no. 4, pp. 1992–2002, Nov 2014.

[3] A. Fadel and B. Zhou, "An experimental and analytical comparison study of power management methodologies of fuel cell–battery hybrid vehicles," *J. Power Sources*, vol. 196, no. 6, pp. 3271–3279, 2011.

[4] S. F. Tie and C. W. Tan, "A review of energy sources and energy management system in electric vehicles," *Renew. and Sustain. Energy Rev.*, vol. 20, pp. 82–102, 2013.


TABLE VIII
CONTROL PERFORMANCE

| | JC08 | | HWFET | |
|---|---|---|---|---|
| | Simulation | Experiment | Simulation | Experiment |
| $F_1$ | 88 % | 88.05 % | 87.6 % | 83.12% |
| $F_2$ | 8.0748 | 7.6877 | 21.9288 | 12.924 |
| $F_3$ | 0.0506 | 0.0525 | 0.018 | 0.011 |

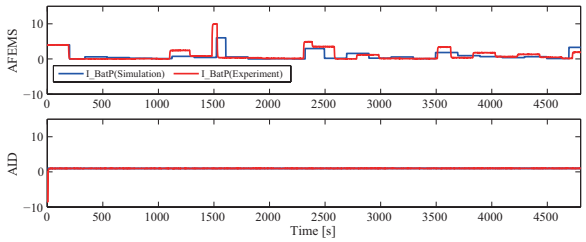


(a)

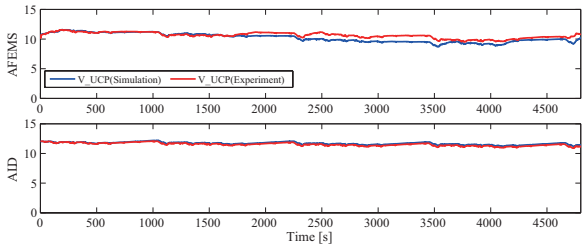


(b)

Fig. 20. Simulation and experimental results for JC08. (a) Current plot. (b) Voltage plot.


[5] K. Ç. Bayindir, M. A. Gözüküçük, and A. Teke, "A comprehensive overview of hybrid electric vehicle: Powertrain configurations, powertrain control techniques and electronic control units," *Energy Convers. Manage.*, vol. 52, no. 2, pp. 1305–1313, 2011.

[6] J. Wu, C.-H. Zhang, and N.-X. Cui, "Fuzzy energy management strategy for a hybrid electric vehicle based on driving cycle recognition," *Int. J. Autom. Technol.*, vol. 13, no. 7, pp. 1159–1167, 2012.

[7] X. W. Gong, C. Gao, and P. Wang, "Development of a novel torque


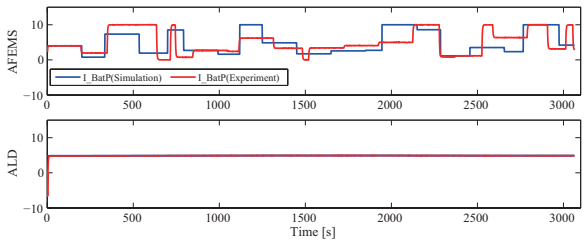


(a)

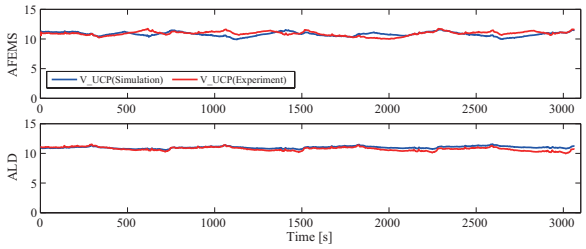


(b)

Fig. 21. Simulation and experimental results for HWFET. (a) Current plot. (b) Voltage plot.

management strategy for parallel hybrid electric vehicle," in *Applied Mechanics and Materials*, vol. 278. Trans Tech Publ, 2013, pp. 1729–1736.

[8] H. Dai, P. Guo, X. Wei, Z. Sun, and J. Wang, "Anfis (adaptive neuro-fuzzy inference system) based online soc (state of charge) correction considering cell divergence for the ev (electric vehicle) traction batteries," *Energy*, vol. 80, pp. 350–360, 2015.

[9] A. A. Abdelsalam and S. Cui, "A fuzzy logic global power management strategy for hybrid electric vehicles based on a permanent magnet electric variable transmission," *Energies*, vol. 5, no. 4, pp. 1175–1198, 2012.

[10] S. G. Li, S. Sharkh, F. C. Walsh, and C.-N. Zhang, "Energy and battery management of a plug-in series hybrid electric vehicle using fuzzy logic," *IEEE Trans. Veh. Technol.*, vol. 60, no. 8, pp. 3571–3585, 2011.

[11] H. Hemi, J. Ghouili, and A. Cheriti, "A real time fuzzy logic power management strategy for a fuel cell vehicle," *Energy Convers. Manage.*, vol. 80, pp. 63–70, 2014.

[12] Q. Li, W. Chen, Y. Li, S. Liu, and J. Huang, "Energy management strategy for fuel cell/battery/ultracapacitor hybrid vehicle based on fuzzy logic," *Int. J. Electr. Power Energy Syst.*, vol. 43, no. 1, pp. 514–525, 2012.

[13] F. Odeim, J. Roes, L. Wülbeck, and A. Heinzel, "Power management optimization of fuel cell/battery hybrid vehicles with experimental validation," *J. Power Sources*, vol. 252, pp. 333–343, 2014.

[14] S. Dusmez and A. Khaligh, "A supervisory power-splitting approach for a new ultracapacitor–battery vehicle deploying two propulsion machines," *IEEE Trans. Ind. Informat.*, vol. 10, no. 3, pp. 1960–1971, 2014.

[15] D. Ahmed Masmoudi, M. Michalczuk, B. Ufnalski, and L. M. Grzesiak, "Fuzzy logic based power management strategy using topographic data for an electric vehicle with a battery-ultracapacitor energy storage," *COMPEL: The International Journal for Computation and Mathematics in Electrical and Electronic Engineering*, vol. 34, no. 1, pp. 173–188, 2015.

[16] K. M. Passino, S. Yurkovich, and M. Reinfrank, *Fuzzy control*. Citeseer, 1998, vol. 42.

[17] A. Kuperman and I. Aharon, "Battery-ultracapacitor hybrids for pulsed current loads: A review," *Renew. and Sustain. Energy Rev.*, vol. 15, no. 2, pp. 981–992, 2011.

[18] H. Yin, C. Zhao, M. Li, and C. Ma, "Utility function-based real-time control of a battery ultracapacitor hybrid energy system," *IEEE Trans. Ind. Informat.*, vol. 11, no. 1, pp. 220–231, 2015.

[19] S. Ebbesen, P. Elbert, and L. Guzzella, "Battery state-of-health perceptive energy management for hybrid electric vehicles," *IEEE Trans. Veh. Technol.*, vol. 61, no. 7, pp. 2893–2900, 2012.

[20] M. Wens and M. Steyaert, *Basic DC-DC Converter Theory*. Springer, 2011.

[21] A. Fotouhi and M. Montazeri-Gh, "Tehran driving cycle development using the k-means clustering method," *Scientia Iranica*, vol. 20, no. 2, pp. 286–293, 2013.

[22] S. J. Moura, H. K. Fathy, D. S. Callaway, and J. L. Stein, "A stochastic optimal control approach for power management in plug-in hybrid electric vehicles," *IEEE Trans. Control Syst. Technol.*, vol. 19, no. 3, pp. 545–555, 2011.

[23] E. 1), *Dynamometer Drive Schedules*, Available: http://www.epa.gov/nvfel/testing/dynamometer.htm, 2007.

[24] O. Laldin, M. Moshirvaziri, and O. Trescases, "Predictive algorithm for optimizing power flow in hybrid ultracapacitor/battery storage systems for light electric vehicles," *IEEE Trans. Power Electron.*, vol. 28, no. 8, pp. 3882–3895, 2013.

[25] M.-E. Choi, S.-W. Kim, and S.-W. Seo, "Energy management optimization in a battery/supercapacitor hybrid energy storage system," *IEEE Trans. Smart Grid*, vol. 3, no. 1, pp. 463–472, 2012.

[26] A. Kuperman, I. Aharon, S. Malki, and A. Kara, "Design of a semi-active battery-ultracapacitor hybrid energy source," *IEEE Trans. Power Electron.*, vol. 28, no. 2, pp. 806–815, 2013.

[27] Netlogo [Online] Available: http://ccl.northwestern.edu/netlogo/.

[28] M. Richter, S. Zinser, M. Stiegeler, M. Mendes, and H. Kabza, "Energy management for range enlargement of a hybrid battery vehicle with battery and double layer capacitors," in *Power Electronics and Applications (EPE 2011), Proceedings of the 2011-14th European Conference on*. IEEE, 2011, pp. 1–6.

[29] N. Jalil, N. A. Kheir, and M. Salman, "A rule-based energy management strategy for a series hybrid vehicle," in *American Control Conference, 1997. Proceedings of the 1997*, vol. 1. IEEE, 1997, pp. 689–693.

**He Yin** (S'13) received the B.S. degree in the electrical and computer engineering from University of Michigan-Shanghai Jiao Tong University Joint Institute, Shanghai Jiao Tong University, Shanghai, China in 2012. He is currently working toward Ph.D. degree in the same institute.

His research interests include optimization and decentralized control of hybrid energy systems and wireless power transfer systems.

**Wenhao Zhou** (S'13) received the B.S. degree and the M.S. degree both in the electrical and computer engineering from University of Michigan-Shanghai Jiao Tong University Joint Institute, Shanghai Jiao Tong University, Shanghai, China in 2012 and 2015, respectively. Currently, he works as an engineer in United Automotive Electronic Systems Co., Ltd, Shanghai, China.

His research interests include the energy management in hybrid electric vehicles.

**Chen Zhao** (S'14) received the B.S. degree from East China University of Science and Technology, Shanghai, China, in 2011. He is currently working toward Ph.D. degree in control science and engineering, University of Michigan-Shanghai Jiao Tong University Joint Institute, Shanghai Jiao Tong University, Shanghai, China.

His research interests include modeling and testing of lithium-ion batteries and control of battery-ultracapacitor energy systems.

**Mian Li** currently is an associate professor in the University of Michigan-Shanghai Jiao Tong University Joint Institute, adjunct associate professor at the school of mechanical Engineering, at Shanghai Jiao Tong University, Shanghai, China. He received his Ph.D. degree from the Department of Mechanical Engineering, University of Maryland at College Park in December 2007 with the Best Dissertation Award. He received his BE (1994) and MS (2001) both from Tsinghua University, China. At the University of Michigan-Shanghai Jiao Tong University Joint Institute, his research work has been focused on robust/reliability based multidisciplinary design optimization and control, including topics such as multidisciplinary design optimization, robust/reliability control, sensitivity analysis, and system modeling.

**Chengbin Ma** (M'05) received the B.S.E.E. (Hons.) degree from East China University of Science and Technology, Shanghai, China, in 1997, and the M.S. and Ph.D. degrees both in the electrical engineering from University of Tokyo, Tokyo, Japan, in 2001 and 2004, respectively.

He is currently a tenure-track assistant professor of electrical and computer engineering with the University of Michigan-Shanghai Jiao Tong University Joint Institute, Shanghai Jiao Tong University, Shanghai, China. He is also with a joint faculty appointment in School of Mechanical Engineering, Shanghai Jiao Tong University. Between 2006 and 2008, he held a post-doctoral position with the Department of Mechanical and Aeronautical Engineering, University of California Davis, California, USA. From 2004 to 2006, he was a R&D researcher with Servo Laboratory, Fanuc Limited, Yamanashi, Japan. His research interests include networked hybrid energy systems, wireless power transfer, and mechatronic control.